View metadata, citation and similar papers at core.ac.uk

brought to you by CORE

provided by Periodica Polytechnica (Budapest University of Technology and Economics)

Periodica Polytechnica Mechanical Engineering

59(1), pp. 1-7, 2015
DOI: 10.3311/PPme.7049
Creative Commons Attribution

RESEARCH ARTICLE

Received 23 September 2013; accepted after revision 08 September 2014

On the Static Instability of Liquid Poppet Valves

Csaba Bazsó[1]*, Csaba Hős[1]

Abstract

This paper focuses on flow induced static instabilities occurring in poppet valves. Computational fluid dynamics simulation were performed to gain static characteristics of the poppet valve and to demonstrate the unstable behaviour of the valve. Based on theoretical considerations, a necessary condition for the stable operation is derived. The study indicates that stability can be obtained with proper geometrical design of the valve or by limiting the total compression of the spring. The paper discusses the possible steps to prevent instability and proper spring selection.

Keywords

application of momentum theory, flow induced instability, force coefficient, static instability

[1] Department of Hydrodynamic Systems, Faculty of Mechanical Engineering, Budapest University of Technology and Economics, H-1521 Budapest, Hungary

* Corresponding author, e-mail: csaba.bazso@hds.bme.hu

1 Introduction

Poppet valves are known to possess stability issues, both static [9,10,18,13] and dynamic ones [9,10,6,12,7]. The analysis of these issues require first of all the static characteristics e.g. discharge or thrust. Several studies concerned with static and dynamics characteristics of poppet valves such as discharge or thrust. Besides this a number of different approaches have been taken by various researchers for investigating the dynamic behaviour of poppet valves and instabilities occurring in valve systems.

The first comprehensive discussion of the possible causes of valve instabilities was reported by [5], suggesting that instabilities can be induced as a result of

a) the interaction between the poppet and other elements
b) flow transition from laminar to turbulent during opening and closing,
c) a negative restoring force,
d) hysteresis of the fluid force, and
e) fluctuating supply pressure.

This paper focuses on instabilities of type c). Type of problem a) has been widely investigated for example in [8,16,6,7], nonlinear response due to e) has been studied for example in [8,14]. Instabilities due to b), c), and d) have been analysed for example in [9,10,11,18,13,15], however, there has been little discussion about the prediction of the stable operation rang and the prevention of the instabilities.

Determination of static characteristics such as discharge coefficient and fluid force is of primary importance in the investigation of flow induced instabilities of poppet valves. Many studies addressed the problem developing analytical formulae and it was concluded that the thrust on a conical poppet valve with chamfered seat exerted by the fluid flow can be easily derived from momentum theory with several simplification, e.g. assuming steady, incompressible and frictionless flow and uniform inlet velocity distribution. Unfortunately, these analytical estimations are limited to simple geometries with several assumptions and these studies do not consider the influence of the developed flow pattern in the downstream chamber.

Experiments published in [11,18] have revealed, that the flow pattern has a great influence on the fluid force. The dominating effect is the jet through the gap that drives usually small vortices into the chamber causing high velocities and low pressures on the poppet face.

Recently, computational fluid dynamics (CFD) techniques provide a reasonable option to understand the fluid mechanical relationships inside a valve and to obtain reliable data on static (see e.g. [4]) and even dynamic characteristics (see e.g. [3,1]) of the valve. The present study also engaged to employ CFD simulations to determine the needed static characteristics.

This study aimed at investigating the flow induced static instability of liquid poppet valves and to provide recommendations for valve design to avoid this type of loss of stability.

Figure 1 shows the sketch of the poppet valves being in focus of interest.

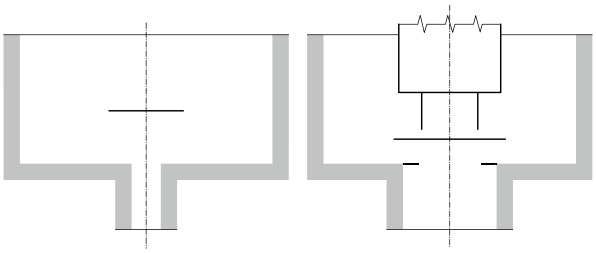

Fig. 1 Sketch of the poppet valves under analysis.

The left configuration investigated by the author of this paper in [2,1] serves as a validation case for the CFD model and later on we refer to this as valve A. The right configuration (taken from Vaughan [18]) constitutes the main objective of the paper and we refer to this as valve B. Both valves are of conical valve body, but the right one includes a flange at the bottom part of the cone. This flange is aimed at deflecting the jet to radial direction thus decreasing the influence of the momentum flux on the axial force balance. However, as it was reported also by Vaughan in [18], sudden change in the flow pattern may occur upon varying the lift giving rise to discontinuities in the static characteristics and leading to unreliable performance of the poppet valve. This observation encouraged the authors of the current paper to explore the effect of the sudden change in the static characteristics on the stability and to make an attempt to predict the range of stable operation.

1.1 Theoretical background

Let us consider a poppet valve with a conical valve body and sharp seat as illustrated in the left panel of Fig. 2. Let α denote the half cone angle of the poppet, D_{seat} the seat diameter, x the lift of the valve body, and $h = x \sin \alpha$ the gap between the poppet and the seat. The inlet area A_1 is the cross-sectional area of the seat $(A_1 = D_{\text{seat}}^2 \pi / 4)$, while the outlet area $A_2(x)$ through the gap can be calculated for small lifts as

$$A_2(x) = D_{\text{seat}} \pi h = D_{\text{seat}} \pi \sin(\alpha) x := c_1 x \tag{1}$$

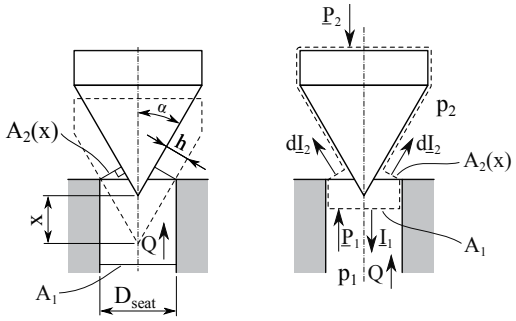

Fig. 2 Left: Representation of the geometrical quantities used in the current paper. Right: Momentum theory applied on the test geometry.

The flow rate Q through the poppet valve (assuming incompressible turbulent flow) is given by the usual discharge formula (see e.g. [8])

$$Q = C_d A_2(x) \sqrt{\frac{2\Delta p}{\rho}}, \quad \text{with} \quad \Delta p = p_1 - p_2 \tag{2}$$

where C_d is the discharge coefficient, p_1 and p_2 are the absolute pressure at the upstream and downstream side of the poppet valve, respectively, and ρ is the density of the working medium, assumed to be constant.

To obtain the force exerted by the fluid we apply the momentum theory on the control volume as it is demonstrated in Fig. 2. The axial component of the momentum equation takes the form

$$-I_1 + I_2 \cos\alpha = P_1 - P_2 - F_{\text{fluid}} \tag{3}$$

where I_1 and I_2 denotes the momentum flux of the flow entering and leaving the control volume, P_1 and P_2 constitutes the net force due to pressure distribution at the upstream and downstream side of the control volume, while F_{fluid} stands for the force exerted by the fluid on the valve. As [17] pointed out, the pressure forces can be expressed simply by $P_1 = A_1 p_1$, and $P_2 = A_1 p_2$, while the momentum flux terms can be assumed to be $I_1 = Q^2\rho/A_1$, $I_2 = Q^2\rho/A_2(x)$. Substituting these terms into (3) the fluid force becomes

$$F_{\text{fluid}} = A_1(p_1 - p_2) + Q^2\rho\left(\frac{1}{A_1} - \frac{\cos\alpha}{A_2(x)}\right). \tag{4}$$

By making use of (2) it can be concluded, that as the lift approaches to zero the momentum term tends also to zero

$$\begin{aligned} &\lim_{x\to\infty} Q^2\rho\left(\frac{1}{A_1} - \frac{\cos\alpha}{A_2(x)}\right) \\ &= \lim_{x\to\infty} \rho\left(C_d A_2(x)\sqrt{\frac{2\Delta p}{\rho}}\right)^2 \\ &\times\left(\frac{1}{A_1} - \frac{\cos\alpha}{A_2(x)}\right) = 0 \end{aligned} \tag{5}$$

that shows that the force needed to open the valve comes purely from the pressure force balance as follows

$$\lim_{x\to\infty} F_{\text{fluid}} = A_1(p_1 - p_2). \tag{6}$$

To give more generality for the findings, the results are presented in terms of non-dimensional quantities, flow coefficient (C_f) and non-dimensional lift (X). The force coefficient is produced by dividing the fluid force by the force derived from the pressure distribution.

$$C_f := \frac{F_{fluid}}{A_1(p_1 - p_2)} \tag{7}$$

while X is defined as

$$X = \frac{x}{D_{\text{seat}}}. \tag{8}$$

As consequence of (6), we have

$$\lim_{x\to\infty} C_f = 1. \tag{9}$$

$C_f < 1$ supposes such flow conditions, that the net momentum flux decreases the total force acting on the poppet valve, while $C_f > 1$ states that the momentum flux increases the fluid force.

2 Computational Fluid Dynamics (CFD) model

The commercial CFD package ANSYS CFX 14 and ICEM CFX meshing software is an effective way to investigate the fluid flow in the flow domain of the valve and to determine static characteristics such as force coefficient, or discharge coefficient. To do this a series of geometries was generated corresponding to different valve lifts. For a prescribed inlet and outlet pressure the resulted fluid force was extracted directly from the CFD results. To validate the CFD settings, the force coefficient was determined analytically for valve A.

The geometry of the two configurations are shown in Fig. 3 and Fig. 4. To develop appropriate velocity profile in the seat region $10D_{\text{seat}}$ long upstream section was used while to avoid recirculation at the outlet a relatively long downstream section was used in each case. To accelerate the computations, axisymmetric geometry was built with angle of 10°. The meshing was designed to provide satisfactory resolution in the crucial region around the poppet, while the density of the mesh was reduced as the gradients of the flow variables decrease. Inlet and opening boundary conditions were employed with prescribed pressure at the inlet (denoted by IN) and outlet (OUT), respectively, on the walls (WALL) and the valve body (VALVE) standard no-slip wall boundary condition was set, while on the sidesurfaces S1 and S2 symmetry boundary condition was applied. The liquid was standard mineral oil ($\rho = 870$ kg/m^3 and $\nu = 40$ mm^2/s). The turbulence was modelled with standard $k - E$ model.

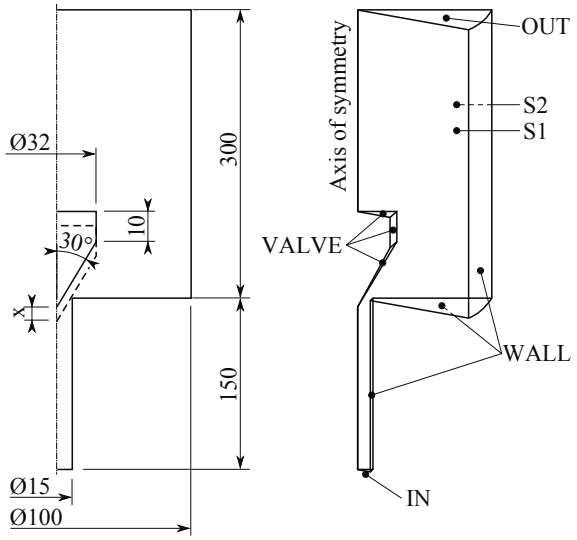

Fig. 3 Geometry of valve A and its 2-D axisymetric flow domain.

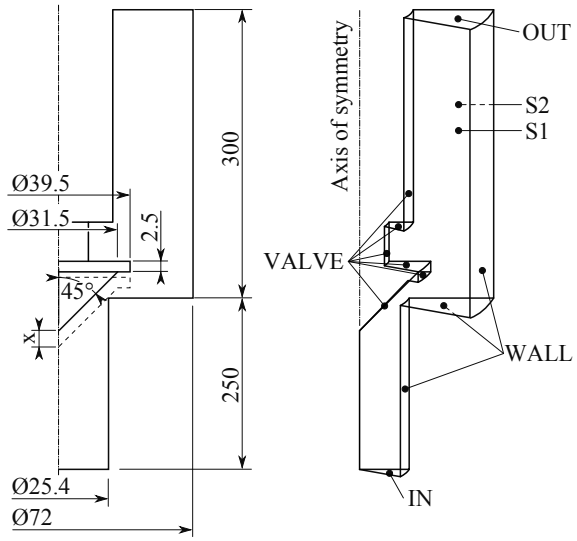

Fig. 4 Geometry of valve B and its 2-D axisymetric flow domain.

3 Results

Two series of simulations were carried out on both valves to investigate the evolving flow pattern and the change of the force coefficient as a function of the lift in the range of $X = x/D_{\text{seat}} = 0 - 0.2$. The pressure difference between the inlet and outlet ($\Delta p = p_1 - p_2$) was $\Delta p = 5$ bar and $\Delta p = 10$ bar, respectively.

To establish the connection with the measurements reported in [2] let us demonstrate the variation of the resulted flow quantities flow rate Q, fluid velocity v_{fl} in the upstream passage and the here defined Reynolds number $\text{Re} = v_{fl} \times D_{seat} / \nu$ for the measurements and simulations studying Table 1. Note, in the case of experiments the given values are only to indicate the magnitude of the accessible maximum values. Moreover, it is worth mentioning that measurements were performed somewhat differently than simulations. In the case of simulations the pressure was kept constant and for a given displacement we obtained a particular flow rate value while in the case of measurement for a prescribed set pressure the flow rate was varied

Table 1 The variation of the resulted flow rate, fluid velocity and Reynolds number ranges in the case of experiments and CFD simulations.

Valve geom.		X [−]	Δp [bar]	Q [l/min]	v_{fl} [m/s]	Re [−]
Valve A, experiments	min	~ 0	~ 0	~ 0	~ 0	~ 0
	max	~ 0.025	~ 18	~ 24	~ 2.2	~ 2400
Valve A, CFD	min	0.025	5	14.58	1.376	516
	max	0.2	10	158.5	14.95	5606
Valve B, CFD	min	0.025	5	63.9	2.104	1336
	max	0.2	10	612	20.07	12745

as parameter resulting in the change of the system pressure and the lift of the valve body. In the case of measurement the working medium was oil with $\rho = 870$ kg/m^3 and $\nu = 37$ mm^2/s.

3.1 Valve A

The developed flow pattern is demonstrated by plotting the velocity magnitude in Fig. 5. As it can bee seen the jet leaving the gap attaches to the poppet valves both for small (a) and high (b) lifts. Neither recirculation in the region of seat nor sudden jump in the flow pattern occurs.

Figure 6 depicts the variation of force coefficient C_f as a function of the nondimensional lift X. As the values of C_f for the two series showed little variance (merely in their third digits), only the results obtained for $\Delta p = 5$ bar are presented. Moreover, the measurement results of [2] and analytical estimation are also represented in the figure. Crosses show the points obtained by CFD simulation, plus sign depicts the measurement results while squares represents the one calculated from (4).

Although the range of measurement of [2] was only $X = 0 - 0.025$ and the method of obtaining C_f was different we can observe a reasonable coincidence. Moreover, the analytical estimation shows satisfying agreement both with measurement and simulation. The error appears to increase for higher lift, yet the maximum error between the two results is less than 2.4%. Motivated by this agreement we have been inclined to apply the above reported settings for further CFD simulations.

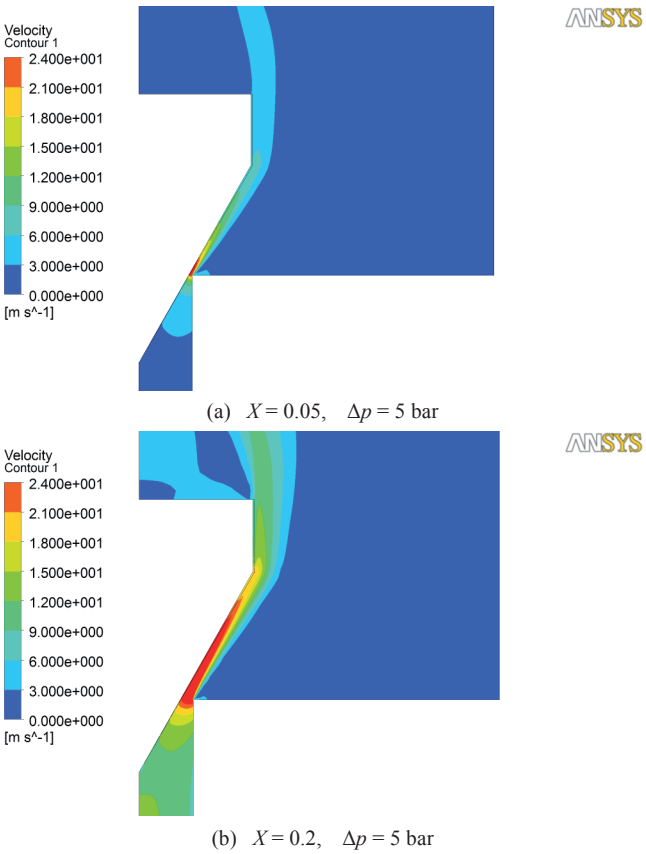

(a) $X = 0.05$, $\Delta p = 5$ bar

(b) $X = 0.2$, $\Delta p = 5$ bar

Fig. 5 Variation of the flow pattern in the case of valve A.

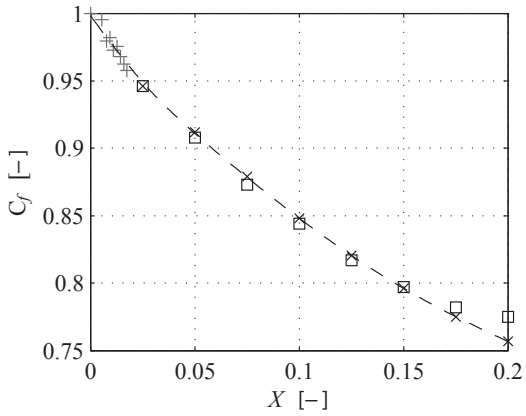

Fig. 6 The force coefficient in case of valve A. Crosses show the points obtained by CFD simulation while dashedline seeks to predict possible shape of the function between the computed points. Squares represent the points gained analytically. Plus sign depicts the measurement results of [2].

3.2 Valve B

Figure 7 represents the flow pattern of valve B for several lifts. It is clearly seen, that for small lifts (a) the flange deflects the jet towards the seat attaching to the seat face, separating and driving a recirculation zone at the inner part of the seat. The jet leaving this region then attaches to the wall of the chamber. Increasing the valve lift the attaching point of the jet to the seat moves outwards along the seat face and then upwards along the wall of the chamber. The direction of the deflection then changes upwards at $X \approx 0.14$. It is worth noting, that between $X \approx 0.12$ (when the jet is redirected straight toward the outer edge) and $X \approx 0.135$ (when the jet is redirected exactly radially toward the wall of the chamber) the flow patterns seemed to be very unstable that coincides with the experimental Vaughan's et al. observation reported in [18].

Figure 8 depicts the variation of force coefficient C_f as a function of the lift. The force coefficient sets off from $C_f = 1$ at $X = 0$ and gradually decreases up to $X \approx 0.75$ where it reaches its minimum value ($C_f = 0.833$). Then the curve increases very slightly up to $X \approx 0.12$ where a steep rise can be observed followed by a regressive but still rising section arriving to $C_f = 1.276$ at $X = 0.2$. As one can see, notable discrepancy can be

(a) $X = 0.05$, $\Delta p = 5$ bar

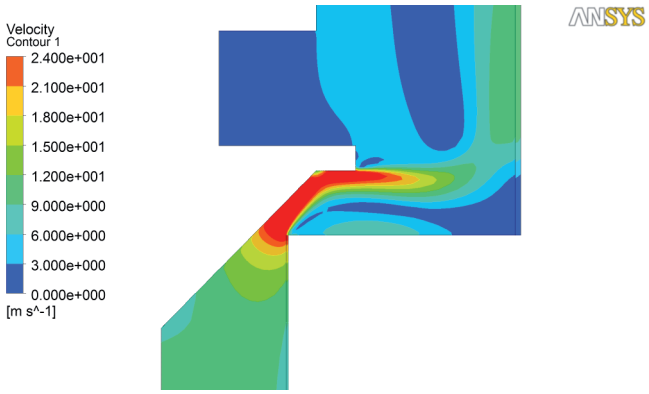

(b) $X = 0.135$, $\Delta p = 5$ bar

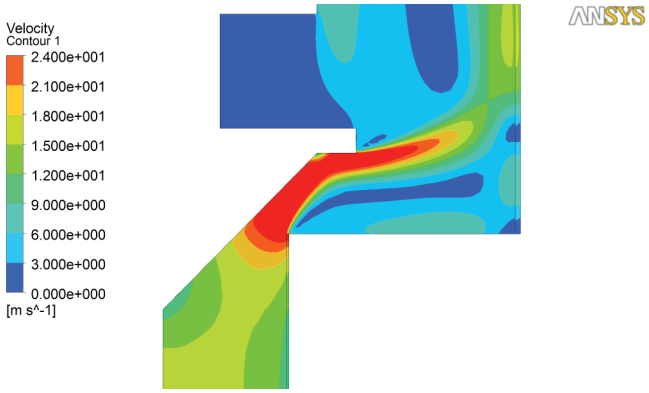

(c) $X = 0.2$, $\Delta p = 5$ bar

Fig. 7 Variation of the flow pattern in the case of valve B.

observed in the variation of the force coefficient compared with the one exhibited by valve A. This is assigned to the diverse topology of the flow pattern in function of the valve lift developed in the downstream chamber as indicated in Fig. 7. Whereas in the case of valve A (see Fig. 5) the jet attaches to the valve body and thus momentum flux is parallel to the poppet face, in the case of valve B the flow is deflected by the flange leading to lift-dependent jet angle and giving rise to a jet-driven recirculating zone on the seat side of the flow domain. The developed vortex reacts back on the poppet face involving the force balance becoming more complex and less predictable. As consequence of this fact no intention was made to estimate analytically the value of the fluid force and force coefficient.

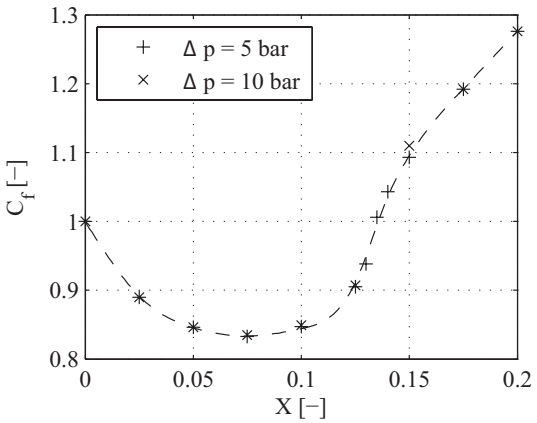

Fig. 8 The force coefficient in case of valve A. Crosses and plus signs show the points obtained by CFD simulation while dashed-line seeks to predict possible shape of the function between the computed points.

4 Static instability

The sudden change in the flow pattern may significantly affect both the discharge coefficient and force coefficient even exhibiting discontinuity or hysteresis leading to undesired behaviour of the valve. Hence a need has arisen to study the effect of fluid force on the stability of the poppet valve.

Let us consider Newton's second law applied on a poppet valve with mass m, viscous damping k, spring coefficient s and spring pre-compression x_0, given by

$$m\ddot{x} + k\dot{x} + s(x + x_0) = F_{\text{fluid}}. \tag{10}$$

Using $F_{\text{fluid}} = C_f \Delta p A_1$, (10) can be rewritten as

$$\dot{x} = v \tag{11}$$

$$\dot{v} = \frac{1}{m}(C_f(x)\Delta p A_1 - s(x + x_0) - kv \tag{12}$$

Close to the equilibrium the dynamics is governed by the eigenvalues of the linear coefficient matrix given by

$$\mathrm{J} = \begin{pmatrix} 0 & 1 \\ \mu & \eta \end{pmatrix} \tag{13}$$

where

$$\mu = -\frac{1}{m}\underbrace{(s - C_f' \Delta p A_1)}_{s_{\text{eff}}}, \qquad \eta = -\frac{k}{m}, \tag{14}$$

representing s_{eff} an effective spring constant. Note, that s_{eff} may become negative leading to static stability loss of the valve.

Considering that for steady state $C_f(x)\Delta p A_1 = s(x + x_0)$, μ can be rewritten as

$$\mu = \frac{s}{m}\left(\frac{C_f'(x)}{C_f(x)}(x + x_0) - 1\right). \tag{15}$$

The eigenvalues are the roots of the characteristic polynomial

$$\det(\mathrm{J} - \lambda\,\mathrm{I}) = \lambda^2 - \eta\lambda - \mu = 0. \tag{16}$$

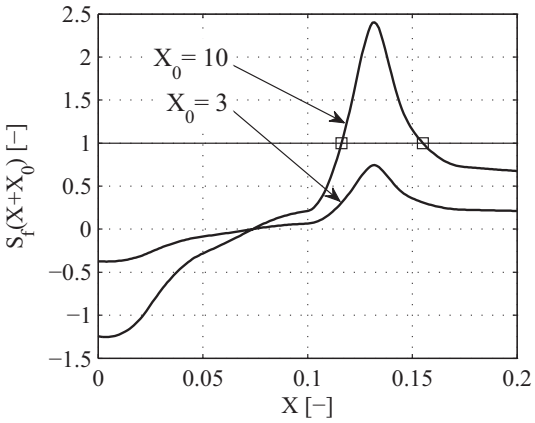

Fig. 9 Variation of $S_f(X+X_0)$ as function of X. $X_0 = 3$ represents an example that fulfils the necessary condition for stability, while $X_0 = 10$ the equilibrium is unstable between $0.1162 < X < 0.155$.

Thus the roots are

$$\lambda_{1,2} = \frac{1}{2}\left(\eta \pm \sqrt{\eta^2 + 4\mu}\right). \tag{17}$$

Notice that a zero eigenvalue occurs if the term inside the square root is equal to η, i.e $\mu = 0$. If this term is less than k/m then both eigenvalues are negative. Hence, a necessary condition for stable operation is

$$\mu < 0 \qquad \rightarrow \qquad \frac{C_f'}{C_f}(x + x_0) < 1 \tag{18}$$

Multiplying the left hand side of the expression by D_{seat}/D_{seat} yields a dimensionless form of the condition

$$S_f(X + X_0) < 1 \tag{19}$$

where $S_f = C_f' / C_f \times D_{seat}$ represents a dimensionless hydrodynamic spring coefficient, $X_0 = x_0/D_{seat}$ denotes the dimensionless spring pre-compression, while $X = x/D_{seat}$ denotes the dimensionless valve lift as defined before. Investigation of (19) indicates that the necessary condition for stable operation is function of two separate factor S_f, being affected purely on geometrical consideration of the valve, and $(X + X_0)$ that is the total compression of the spring being independent of the set pressure and spring constant. As $(X + X_0)$ is always positive the condition can be met by keeping $S_f = C_f' / C_f \times D_{seat} \leq 0$. D_{seat} is always positive and due to the nature of the force balance on the poppet valve C_f may be positive (see (9)). Thus the most practical way to attain $S_f \leq 0$ is to design such valve geometry that satisfies $C_f' \leq 0$, in other words to provide the derivative of the force coefficient to never become positive. Consequently, as valve A exhibits monotonous decreasing C_f characteristics, it always satisfies condition (19). Consisting increasing C_f characteristic, valve B may fulfil condition (19) depending on how much total compression $(X + X_0)$ the spring is subject to. This is demonstrated in Fig. 9. Whereas for $X_0 = 3$ the condition is met being $S_f(X + X_0) < 1$, for $X_0 = 10$ the condition is not fulfilled between $0.1162 < X < 0.155$ being $S_f(X + X_0) > 1$.

5 Recommendations for valve design

The above findings can be used in practical valve design as follows.

(i) In the design phase such a valve geometry is recommended to be developed whose force coefficient characteristics is monotonous decreasing upon increasing the valve lift.
It is worth mentioning that a real flow may exhibit hysteresis during opening and closing the valve, thus caution need to be applied when performing experiments or CFD simulations on determining the force coefficient C_f.

(ii) If the geometry is already given and the hydrodynamic spring coefficient becomes positive under varying the lift, the following steps are supposed to be taken to meet condition (19).
Poppet relief valves are designed for a maximum capacity (Q_{max}) opening at a prescribed set pressure (p_{set}). Assuming monotonous increasing discharge coefficient C_d in function of the valve lift, the maximum lift corresponds to the maximum flow rate, thus its value can be determined from (2) as follows

$$x_{max} = \frac{Q_{max}}{C_d c_1 \sqrt{\frac{2p_{set}}{\rho}}}, \qquad \rightarrow \qquad X_{max} = \frac{x_{max}}{D_{seat}}. \tag{20}$$

In the knowledge of S_f obtained from measurement or CFD simulation the admissible maximum spring pre-compression is calculated from (19) as

$$X_{0,max} < \frac{1}{\max S_f} - X_{max,} \qquad \rightarrow$$
$$\rightarrow x_{0,max} = X_{0,max} D_{seat}. \tag{21}$$

Thus the spring constant needed to satisfy condition (19) is

$$s_{min} > \frac{p_{set} A_1}{x_{0,max}}. \tag{22}$$

6 Conclusion

Computational fluid dynamics simulations were performed to gain static characteristics of poppet valves. Investigation of the influence of the force coefficient C_f on the valve performance revealed that the effective spring constant may become negative leading to static stability loss of the valve. Based on linear stability analysis the necessary condition for stable operation was determined. Moreover, it was shown that the condition is function of two separate effects, the hydrodynamic spring constant and the total compression of the spring. It was concluded that the stability can be obtained either by providing $S_f \leq 0$ or holding the total compression of the valve sufficiently low and selecting less stiff spring for a given purpose.

Acknowledgement

This research was supported by the János Bolyai research grant of the Hungarian Academy of Sciences of C. Hős. Moreover, the authors would like to express their thanks to Mihály Gráf, MSc student of the Budapest University of Technology and Economics, for giving them assistance performing the CFD simulations.

References

[1] Bazsó, C., Hős, C. J. "A CFD study on the unsteady forces on a hydraulic poppet valve." In: *Proceedings of Conference on Modelling Fluid Flow.* 2012.

[2] Bazsó, C., Hős, C. J. "An experimental study on the stability of a direct spring loaded poppet relief valve." *Journal of Fluids and Structures*. 42. pp. 456-465. 2013. DOI: 10.1016/j.jfluidstructs.2013.08.008

[3] Beune, A. "*Analysis of high-pressure safety valves*." PhD thesis. Eindhoven University of Technology. 2009.

[4] Chabane, S., Plumejault, S., Pierrat, D., Couzinet, A., Bayart, M. "Vibration and chattering of conventional safety relief valve under built up back pressure." In: *Proceedings of the 3rd IAHR International Meeting of the Work-Group on Cavitation and Dynamic Problems in Hydraulic Machinery and Systems*. pp. 281-294. 2009.

[5] Green, W. L., Woods, G. D. "*Some causes of chatter in direct acting spring loaded poppet valve.*" In: The 3rd International Fliud Power Symposium. Turin. 1973.

[6] Hayashi, S. "Nonlinear phenomena in hydraulic systems." In: *Proceedings of the 5th International Conference on Fluid Power Transmission and Control.* 2001.

[7] Hős, C., Champneys, A. R. "Grazing bifurcations and chatter in a pressure relief valve model." *Physica D: Nonlinear Phenomena*. 241 (22). pp. 2068-2076. 2011. DOI: 10.1016/j.physd.2011.05.013

[8] Kasai, K. "On the stability of a poppet valve with an elastic support: 1st report, considering the effect of the inlet piping system." *Bulletin of Japan Society of Mechanical Engineers*. 11 (48). pp.1068-1083. 1968. DOI: 10.1299/jsme1958.11.1068

[9] Madea, T. "Studies on the dynamic characteristic of a poppet valve: 1st report, theoretical analysis." *Bulletin of Japan Society of Mechanical Engineers*.13 (56). pp. 281-289. 1970. DOI: 10.1299/jsme1958.13.281

[10] Madea, T. "Studies on the dynamic characteristics of a poppet valve: 2nd report, experimental analysis." *Bulletin of Japan Society of Mechanical Engineers*. 13 (56). pp. 290-297. 1970. DOI: 10.1299/jsme1958.13.290

[11] Mccloy, D., Mcguigan, R. H. "Some static and dynamic characteristics of poppet valves." In: Proceedings of the Institution of Mechanical Engineers. 179. pp. 199-213. 1964. DOI: 10.1243/pime_conf_1964_179_215_02

[12] Misra, A., Behdinan, K., Cleghorn, W. L. "Self-excited vibration of a control valve due to uid-structure interaction." *Journal of Fluids and Structures.* 16 (5). pp. 649-665. 2002. DOI: 10.1006/jfls.2002.0441

[13] Moussou, P., Gibert, R. J., Brasseur, G., Teygeman, Ch., Ferrari, J., Rit, J. F. "Instability of Pressure Relief Valves in Water Pipes." *Journal of Pressure Vessel Technology.* 132 (4). 041308. 2010. DOI: 10.1115/1.4002164

[14] Nayfeh, A. H., Bouguerra, H. "Non-linear response of a fluid valve." *International Journal of Non-Linear Mechanics.* 25 (4). pp. 433-449. 1990. DOI: 10.1016/0020-7462(90)90031-4

[15] Song, X-G., Park, Y-C., Park, J-H. "Blowdown prediction of a conventional pressure relief valve with a simplified dynamic model." *Mathematical and Computer Modelling.* 57 (1-2). pp. 279-288. 2013. DOI: 10.1016/j.mcm.2011.06.054

[16] Thomann, H. "Oscillations of a simple valve connected to a pipe." *Zeitschrift fur Angewandte Mathematik und Physik*. 27 (1). pp. 23-40. 1976. DOI: 10.1007/bf01595239

[17] Urata, E. "Thrust of poppet valve." *Bulletin of The Japan Society of Mechanical Engineers*. 12 (53). pp. 1099-1109. 1969. DOI: 10.1299/jsme1958.12.1099

[18] Vaughan, N. D., Johnston, D. N., Edge, K. A. "Numerical simulation of fluid flow in poppet valves." *Proceedings of the Institution of Mechanical Engineers.* 206 (2). pp. 119-127. 1992. DOI: 10.1243/pime_proc_1992_206_105_02